

## **General Disclaimer**

### **One or more of the Following Statements may affect this Document**

- This document has been reproduced from the best copy furnished by the organizational source. It is being released in the interest of making available as much information as possible.
- This document may contain data, which exceeds the sheet parameters. It was furnished in this condition by the organizational source and is the best copy available.
- This document may contain tone-on-tone or color graphs, charts and/or pictures, which have been reproduced in black and white.
- This document is paginated as submitted by the original source.
- Portions of this document are not fully legible due to the historical nature of some of the material. However, it is the best reproduction available from the original submission.

**X-662-76-198**

**PREPRINT**

**NASA TM X- 71186**

**FINAL SAS-2  
GAMMA RAY RESULTS  
ON SOURCES IN THE  
GALACTIC ANTICENTER REGION**

(NASA-TM-X-71186) FINAL SAS-2 GAMMA RAY  
RESULTS ON SOURCES IN THE GALACTIC  
ANTICENTER REGION (NASA) 38 p HC \$4.00

**N76-32094**

**CSCI 03B**

**G3/93**

**Unclas  
03267**

**D. J. THOMPSON  
C. E. FICHEL  
R. C. HARTMAN  
D. A. KNIFFEN  
R. C. LAMB**

**AUGUST 1976**



**— GODDARD SPACE FLIGHT CENTER —  
GREENBELT, MARYLAND**

FINAL SAS-2 GAMMA RAY RESULTS ON SOURCES IN THE  
GALACTIC ANTICENTER REGION

D. J. Thompson, C. E. Fichtel, R. C. Hartman, D. A. Kniffen, and  
R. C. Lamb\*

NASA/Goddard Space Flight Center, Greenbelt, Maryland 20771

ABSTRACT

Final analysis of the SAS-2 high energy  $\gamma$ -ray data from the direction of the galactic anticenter shows that this region is characterized by three features: a diffuse emission from the galactic plane which has a maximum along  $b = 0^\circ$  and an enhancement toward negative latitudes associated with Gould's Belt, a strong point source in the direction of the Crab nebula, and a second intense localized source near galactic coordinates  $195^\circ, +5^\circ$ . The principal aspects of these results are:

1. The  $\gamma$ -ray emission from the Crab source is dominated by a pulsed flux from PSR 0531+21. The final analysis shows that the main and interpulses are about equal in the  $\gamma$ -ray energy range. The pulsed and total emissions are consistent with power law spectra connecting to the X-ray data. The total flux above 100 MeV is  $(3.7 \pm 0.8) \times 10^{-6} \text{ cm}^{-2}\text{s}^{-1}$ .
2. The source observed near  $195^\circ, +5^\circ$  has a flux above 100 MeV of  $(4.3 \pm 0.9) \times 10^{-6} \text{ cm}^{-2}\text{s}^{-1}$ . Its spectrum appears flatter than that of the Crab, being consistent with a  $\pi^\circ$  plus bremsstrahlung origin or a flat power law. Unlike other  $\gamma$ -ray sources, no radio counterpart has

\*On faculty leave from Iowa State University.

has been found for  $\gamma 195 +5$ . If this source is due to an undiscovered radio pulsar, the results from other known  $\gamma$ -ray pulsars would suggest a radio intensity of 0.2 to 1.4 Jy. If the  $\gamma$ -rays originate from cosmic ray--matter interactions, radio observations of matter densities would imply a substantially higher cosmic ray intensity at the source than observed locally.

3. The diffuse galactic plane emission at negative latitudes shows a general correlation with the local matter distribution associated with Gould's Belt. The  $\gamma$ -ray intensity calculated using the observed matter distribution and assuming the local cosmic ray spectrum agrees well with the SAS-2 observations.

## I. INTRODUCTION

In the spectral region of energetic ( $E \geq 30$  MeV)  $\gamma$ -rays, the entire galactic plane is significantly more intense than the apparently diffuse radiation from the rest of the sky (Fichtel et al., 1975). However, in the galactic anticenter region the emission from the galactic plane is an order of magnitude smaller than in the central galactic region from  $l \approx 300^\circ$  to  $l \approx 50^\circ$ , where cosmic ray interactions in the major structural features of the inner galaxy appear to play a major role. Hence, there is a better chance of seeing individual features near the galactic plane in the anticenter region. Two localized sources are very clearly evident in the SAS-2 data, and one other location is an interesting candidate for future studies. Further, there is a broad general enhancement  $10^\circ$  to  $15^\circ$  south of the galactic plane in the anticenter region,



relative to the same region north of the plane. This increased intensity is generally correlated with local galactic features. Final results on all of these observations will be presented here together with a discussion of the possible interpretations.

The telescope used to collect the data is a 32-level wire-grid, magnetic-core spark chamber assembly covered by an anticoincidence scintillator and triggered by any one of four independent directional scintillator-Cerenkov counter telescopes in anticoincidence with the outer scintillator. Thin tungsten plates, 0.03 radiation length-thick, are interleaved between the spark-chamber modules, which have an active area of approximately  $640 \text{ cm}^2$ . The large number of thin tungsten plates and spark chambers serve a dual purpose: first, to provide material for the  $\gamma$ -ray to be converted into an electron pair which can then be clearly identified and from which the arrival direction of the  $\gamma$ -ray can be determined; and second, to provide a means of determining the energy of the electrons in the pair by measuring their Coulomb scattering. The full width half maximum field of view is  $35^\circ$ , and within the field of view the average angular uncertainty for determining the arrival direction of an individual  $\gamma$ -ray projected on one plane is about  $2.6^\circ$  at 100 MeV and varies with energy approximately as  $E^{-1/2}$  in the range from 35 to 200 MeV.

The energy threshold is about 30 MeV. The energy of the  $\gamma$ -ray can be measured up to about 200 MeV, and the integral flux above 200 MeV can be determined. A more complete discussion of the SAS-2  $\gamma$ -ray telescope is given by Derdeyn et al. (1972).

## II. DATA ANALYSIS AND RESULTS

A general discussion of the data analysis procedures used for the SAS-2  $\gamma$ -ray experiment, along with a description of the calibration program, is given by Fichtel et al. (1975); hence only those aspects of the data reduction peculiar to the matters of interest in this paper will be given here. The data from which the primary results to be discussed here were deduced were collected during the periods shown in Table 1. With these periods, the longitudinal range mentioned above could be studied and a search for time variations could be made over a significant portion of this region.

Table 1

SAS-2 Observing Period	Dates of Observation	Average Direction of Detector Central Axis			
		$\ell$	$b$	R.A.	Dec.
4	Dec. 14-21, 1972	182°	-3°	84°	25°
5	Dec. 21-28, 1972	190°	-30°	65°	4°
9	Jan. 11-17, 1973	210°	-0°	101°	3°
22	April 17-24, 1973	182°	-3°	84°	25°

The principal point with regard to the data analysis which will be discussed here is the method of estimating the galactic and celestial diffuse intensity which must be subtracted from the intensity observed in the local region of a point source in order to obtain a good estimate of the point source flux and location. The longitude region from  $\ell = 155^\circ$  to  $\ell = 240^\circ$  was used to determine the combined contribution

of the galactic and general celestial diffuse emission as a function of galactic latitude in  $2^\circ$  intervals. A notable characteristic of the combined galactic and celestial diffuse radiation in the general anticenter region is the asymmetry with respect to the galactic plane, with the intensity at negative latitudes being higher than that at comparable positive latitudes, although the maximum intensity is approximately at  $b = 0^\circ$ .

The portion of the regions ( $175^\circ < l < 205^\circ$ ) which was more than  $2\sigma$  away from both the Crab nebula and a second source at  $l = 195^\circ$ ,  $b = +5^\circ$  appeared to have a slightly higher diffuse galactic radiation than either the region with  $l < 175^\circ$  or the region  $l > 205^\circ$ . However, in view of possible source contamination an intermediate value for the diffuse radiation was used, and the estimated uncertainty is such that the range of values within the uncertainty limits at any latitude encompasses the best estimate of both longitude ranges. At larger  $b$  values, the two sets of values merge and the uncertainty is predominantly determined by statistics, not the background level uncertainty. On the basis of the background determination a shift ( $\sim 13\%$ ) in detection efficiency was noted between the first three periods listed in Table 1 and the last one in April, 1973. The calculated intensities from this latter period have been adjusted to reflect this change and the error has been increased accordingly.

A general view of the galactic anticenter as seen by SAS-2 is shown in Fig. 1. This map incorporates the four weeks of observations and shows contours of equal  $\gamma$ -ray intensities above 35 MeV. Although many

of the fluctuations which appear on this map are of low statistical significance, three very statistically significant features do appear. Two are localized sources, one near coordinates  $185^\circ$ ,  $-6^\circ$  associated with the Crab nebula and PSR 0531 +21, and the other near coordinates  $195^\circ$ ,  $+5^\circ$ . The positions of maximum intensity in Fig. 1 are shifted somewhat toward the galactic plane from the best estimates of the source positrons. This shift arises from two factors: (1) the sources are superimposed on the galactic plane emission, which has a maximum at  $0^\circ$  latitude and decreases both above and below the galactic plane causing intensity contours surrounding a source to be closer to  $b = 0^\circ$  than if the diffuse radiation were isotropic, and (2) the smoothing procedure used to generate the contours causes a slight distortion. The third statistically-significant feature visible is the asymmetry with respect to the galactic plane and particularly the general enhancement  $10^\circ$  to  $15^\circ$  south of the galactic plane, which is in the general position of Gould's Belt in this region of the sky. The location of the other possible excess noted earlier is ( $165^\circ$ ,  $-39^\circ$ ) in galactic coordinates.

#### A. Crab Nebula

The Crab nebula, which contains PSR 0531 +21, was the first positively-identified  $\gamma$ -ray source (Browning, Ramsden, and Wright, 1971; Albats et al., 1972; Kinzer, Share, and Seeman, 1973; Parlier et al., 1973; McBreen et al., 1973; Kniffen et al., 1974). The preliminary SAS-2 results on the Crab (Kniffen et al., 1974) were based on only the first of the four observing periods which covered the region. For the analysis reported here, circles were chosen about

the known position of the radio pulsar such that 90% of all the source events would be included. These circles had radii of  $6^\circ$  for  $\gamma$ -rays with energies above 100 MeV,  $9^\circ$  for  $\gamma$ -rays with energies between 60 MeV and 100 MeV, and  $12^\circ$  for  $\gamma$ -rays with energies between 35 and 60 MeV.

The arrival time for each of the 260 chosen  $\gamma$ -rays was converted to a pulsar phase by correcting the time to the solar system barycenter, using the programs previously developed for  $\gamma$ -ray pulsar studies (Thompson et al., 1975; Ugelman et al., 1976). As a check on the procedure, some of the arrival times were compared to radio pulses using predicted arrival times provided by J. M. Rankin of the Arecibo Radio Observatory. The radio comparison also provided an absolute phase prediction for the center of the main pulse.

The results of the phase calculation are shown in Fig. 2. Two peaks are visible, consistent with the positions of the radio main pulse and interpulse. The apparent widths of the peaks are determined by the timing resolution of the detector and the uncertainty in combining data separated in time by 18 weeks. The true pulse widths must be smaller than those shown here, as can be seen in the preliminary results from the COS-B experiment (Bennett et al., 1976). In Fig. 2, the number of  $\gamma$ -rays in the main and interpulses are approximately the same, as seen also in the X-ray data summarized by Helmken (1975). This contrasts with the radio and optical measurements, which show a main peak substantially larger than the interpulse.

In order to obtain an absolute flux for the pulsed component of the emission from the Crab and in order to determine the unpulsed

contribution from the source, the contributions from the diffuse galactic and celestial emission and the source near  $195^\circ$ ,  $+5^\circ$  must be subtracted. The method for calculating the diffuse contributions was described in the previous section. The contribution from the  $195^\circ$ ,  $+5^\circ$  source was estimated from the flux determined for this source, and is less than 5% of the diffuse radiation in the circles used for the Crab analysis. The result, together with its uncertainty, is shown in Fig. 2 as a dashed line.

Taking the pulsed component in this phase plot to cover the ranges 0.95 - 0.15 and 0.35 - 0.60, the remaining bins show some evidence of an excess above the level of the diffuse radiation. For all energies above 35 MeV, the unpulsed Crab component is  $(5.7 \pm 2.9) \times 10^{-6} \text{ cm}^{-2} \text{ s}^{-1}$ , while the pulsed component is  $(8.2 \pm 1.5) \times 10^{-6} \text{ cm}^{-2} \text{ s}^{-1}$ . For energies above 100 MeV, the unpulsed component is  $(0.8 \pm 0.8) \times 10^{-6} \text{ cm}^{-2} \text{ s}^{-1}$ , and the PSR 0531 +21 contribution is  $(2.9 \pm 0.5) \times 10^{-6} \text{ cm}^{-2} \text{ s}^{-1}$ . The total Crab flux above 100 MeV is therefore  $(3.7 \pm 0.8) \times 10^{-6} \text{ cm}^{-2} \text{ s}^{-1}$ . This value agrees with the preliminary SAS-2 results (Kniffen et al., 1974), and that from the COS-B experiment (Bennett et al., 1976).

Over the SAS-2 energy range, these results can be fitted to a power law form. The total flux (pulsed plus constant) from the Crab is given by

$$F_{\text{total}} = (4.68 \pm 0.95) \times 10^{-6} \left( \frac{E}{100} \right)^{-1.25^{+0.40}_{-0.35}} \text{ MeV cm}^{-2} \text{ s}^{-1} \text{ MeV}^{-1}$$

with  $E$  expressed in MeV. The pulsed component can be expressed

$$F_{\text{pulsed}} = (2.87 \pm 0.51) \times 10^{-6} \left( \frac{E}{100} \right)^{-1.00^{+0.60}_{-0.55}} \text{ MeV cm}^{-2} \text{ s}^{-1} \text{ MeV}^{-1}.$$

This pulsed result is shown in Fig. 3 together with other pulsed results from the Crab in the  $\gamma$ -ray energy range. The SAS-2 results are consistent with the total and pulsed energy spectra extrapolated from the X-ray energy range (Laros, Matteson, and Pelling, 1973, and references therein), and with the spectral fit to the pulsed  $\gamma$ -ray data by McBreen et al. (1973). In general, the observations of the Crab pulsed flux are consistent with each other, except possibly in the 5-50 MeV energy range which is characterized by relatively large uncertainties.

Evidence for time variability has been presented by Greisen et al. (1975) at energies substantially above the SAS-2 energy range. Within the relatively limited statistics, the SAS-2 Crab observations show no evidence for variability of either the pulsed or total emission between the 1972 December and 1973 April viewing periods. The pulsed flux above 35 MeV was found to be  $(7.1 \pm 2.2) \times 10^{-6} \text{ cm}^{-2} \text{ s}^{-1}$  in December and  $(9.3 \pm 2.3) \times 10^{-6} \text{ cm}^{-2} \text{ s}^{-1}$  in April. The SAS-2 pulsed result shown in Fig. 3 is consistent with either the 1971 October or the 1973 July results of the Cornell balloon experiment (McBreen et al., 1973; Greisen et al., 1975).

Together with other observations of the Crab, the SAS-2 results presented here reinforce the conclusions reached in the preliminary report (Kniffen et al., 1974). First, the  $\gamma$ -ray observations seem consistent with a continuous extrapolation of the energy spectra measured in the X-ray energy range, for both the pulsed and total emission from the Crab. In light of the power law spectrum and the observed polarization of the X-rays from the Crab (Weisskopf et al.,

1976), synchrotron radiation appears to be the most likely production mechanism for at least the unpulsed part of the  $\gamma$ -ray flux. The detection of a constant flux from the Crab at energies above 35 MeV then implies the existence of electrons with energies in excess of  $10^{15}$  eV in the nebula, assuming a nebular magnetic field of about  $5 \times 10^{-4}$  gauss. Such electrons presumably have their origin in the pulsar.

The most prominent feature of the high-energy results from the Crab is the shift from a predominantly unpulsed flux at X-ray energies (about 10% pulsed below 20 keV; according to the data summarized by Thomas and Fenton, 1975) to a predominantly pulsed flux at  $\gamma$ -ray energies. Within the uncertainties, the SAS-2 measurements are consistent with the flux from the Crab being nearly 100% pulsed above 100 MeV. Assuming that the pulsar is the ultimate source of energy for both the pulsed and unpulsed radiation, this shift is not extremely surprising. Both the particle acceleration and energy loss mechanisms are likely to be much more efficient near the pulsar than in the nebula, allowing the production of higher energy photons within the pulsar magnetosphere than outside. The exact mechanism for production of pulsed  $\gamma$ -rays is uncertain at this time, although it is probably some form of interaction between accelerated electrons and the intense magnetic field surrounding the pulsar.

#### B. $\gamma$ 195 +5

The other strong localized source seen in Fig. 1 has been given the provisional name  $\gamma$ 195+5, corresponding to its approximate galactic coordinates. At this time there is no obvious correlation with any



feature seen at other wavelengths. The source's position, its spectrum, the result of a period search, and efforts at identification will be discussed in turn.

Fig. 4 shows the  $\gamma$ -ray intensity along latitude and longitude strips in the vicinity of the source. The longitude bins are  $2\frac{1}{2}^\circ \times 10^\circ$ ; the latitude bins  $2^\circ \times 10^\circ$ . Because of the better energy resolution associated with higher energy  $\gamma$ -rays, these data, from viewing periods 4 and 8 (see table 1), are restricted to  $\gamma$ -rays whose measured energies are in excess of 100 MeV. Each point represents the net intensity after an estimate of the diffuse galactic and celestial emission has been subtracted. The overall statistical significance of the enhancement when data from all observing periods is considered is approximately  $7\sigma$ . The resulting intensity profiles seen in Fig. 4 can be approximated by one-dimensional Gaussian distributions with widths ( $\sigma$ ) of about  $2.8^\circ$  in longitude and  $2.0^\circ$  in latitude, consistent with the SAS-2 angular resolution for a point source. The means of the two distributions are  $194.9^\circ$  and  $4.9^\circ$ , with a statistical error of about  $\pm\frac{1}{2}^\circ$ . There is an additional uncertainty associated with the shape of the diffuse radiation. For the longitude distribution this uncertainty is relatively small and estimated to be  $\pm\frac{1}{2}^\circ$ . For the latitude distribution, uncertainty in the sharpness of the galactic ridge contributes an estimated error of  $\pm 1^\circ$ . If the two types of errors are summed in quadrature the following position with 95% confidence level error box for the sources is obtained:  $l = 194.9 \pm 1.5^\circ$ ,  $b = 4.9 \pm 2.2^\circ$ . Confirmation of this source for energies greater than 100 MeV has been recently reported by the COS-B collaboration (Bennett et al., 1976).

The spectrum from  $\gamma 195+5$  appears to be somewhat harder than that of other sources, and, therefore, it is appropriate to review briefly the type of energy information which is available from the SAS-2  $\gamma$ -ray detector, although it is discussed in much more detail by Fichtel et al. (1975). Because of the limited statistics and the inherent detector energy resolution function, using a least squares matrix inversion method of unfolding does not lead to meaningful results. On the other hand, if the true spectrum is assumed to be smooth over the energy range of interest (about 25 to 500 MeV), then the experimentally observed distribution can be calculated on the basis of the experimentally measured energy dependent resolution. It is assumed that the true spectrum is either a power law of the form  $dJ/dE = KE^{-\alpha}$  or a cosmic ray nucleon--nucleon interaction  $\gamma$ -ray spectrum as calculated, for example, by Stecker (1970). The energy distribution that will result for these various spectra can then be calculated and compared to the observed distributions. On the basis, the  $\gamma 195+5$  source spectrum is consistent with a combined cosmic ray  $\pi^0$  and bremsstrahlung spectrum of the form produced by the local cosmic rays or a power law spectrum with  $\alpha$  less than 1.9 (95% confidence) below 500 MeV. The flux above 100 MeV depends somewhat on the actual spectral shape, but our best estimate is  $(4.3 \pm 0.9) 10^{-6}$  (photons  $> 100$  MeV)  $\text{cm}^{-2}\text{s}^{-1}$ .

The  $\gamma$ -ray events from the vicinity of  $\gamma 195+5$  have been examined for evidence of periodicity. The total number of  $\gamma$ -rays used, 121, spread over three separate intervals of observation, places a sensible lower limit of about 10 seconds on possible trial periods. No single

period was found consistent among the three sets of data from the three intervals of observation. Because of an apparent regularity in the time between  $\gamma$ -rays from observing period 4 (Dec. 14-21, 1972) in which the time intervals were integer multiples of approximately 58 seconds, a search restricted to a 4 second range around this value was made, with the added freedom that a non-zero time derivative of the period was allowed. A period of 59 s which increased at a constant rate of  $2.2 \times 10^{-9}$  gave the phase plot which is shown in Fig. 5. Also shown in the figure are the phase plots for the individual weeks. In view of the number of trials used and the added degree of freedom in assuming a non-zero time derivative of the period, the evidence for this periodicity is not statistically compelling but is worth examination by future experiments.

In attempting to identify this source we are guided by the previous SAS-2 identifications of localized sources. Four of the SAS-2 sources (Ügelman et al., 1976; Thompson et al., 1976) are identified with radio pulsars (PSR 0531+21, PSR 0833-45, PSR 1747-46, PSR 1818-04) with the first two listed being associated also with relatively young supernova remnants, the Crab nebula (this work) and the Vela SNR (Thompson et al., 1975). If  $\gamma$ 195+5 has a similar nature to these four sources, then within certain limits a prediction of the radio intensity expected from it can be made. Table 2 lists the ratio of the radio emission in the few hundred MHz region to the  $\gamma$ -ray energy flux at 100 MeV for the four pulsar sources and for  $\gamma$ (195,+5).

TABLE 2

<u><math>\gamma</math>-Ray Source</u>	<u>Ratio of Radio Intensity<sup>a</sup> to 100 MeV <math>\gamma</math>-Ray Intensity</u>
Crab pulsar & SNR	$10^{11.8}$ (total, 179 MHz) $10^{8.4}$ (pulsar only, 400 MHz)
Vela pulsar & SNR	$10^{11.4}$ (total, 85 MHz) $10^{8.8}$ (pulsar only, 400 MHz)
PSR 1747-46	$10^{8.1}$ (400 MHz)
FSR 1818-04	$10^{8.0}$ (400 MHz)
$\gamma$ 195+5	$< 10^{9.5}$ (using the strongest radio source within location error box) (179 MHz)

<sup>a</sup>Radio intensities for the pulsars were taken from Taylor and Manchester (1975), the total Crab emission from Bennett (1962), and total Vela emission from Mills et al. (1960)

In order to make this comparison it was necessary to convert the  $\gamma$ -ray intensities to differential energy flux values. Because of uncertainties in the spectral shape of the  $\gamma$ -ray emission this conversion introduces an uncertainty in the ratio of about a factor of 2. An upper limit for  $\gamma$ 195+5 has been calculated by taking the intensity of the strongest radio source within the location error box. This source, 4C+19.22 (e.g. Dixon, 1970) has an intensity at 179 MHz of 7.0 Jy, and the upper limit of  $10^{9.5}$  for the radio/ $\gamma$ -ray ratio follows. This ratio

is approximately two orders of magnitude less than that associated with the Crab and Vela pulsars and their remnants, and apparently rules out a similar origin of the source. Not ruled out, however, is a possible undiscovered pulsar. An interesting feature apparent in Table 2 is the similarity of the four pulsars in which the radio/ $\gamma$ -ray ratio lies in the range of  $10^{8.0}$  to  $10^{8.8}$ . If these values are indicative of the ratio of radio to  $\gamma$ -ray intensities for all radio pulsars, then a radio intensity of 0.2 to 1.4 Jy for a pulsar counterpart of  $\gamma$ 195+5 would follow. It is interesting to note that a previous search for pulsars in this region (Davies, Lyne, and Seiradakis, 1973) was restricted to galactic latitudes of less than  $4^\circ$  (Seiradakis, 1976). A search of the  $\gamma$ 195+5 error box for radio pulsars to the level of 0.1 Jy would be very desirable.

There is one other SAS-2 source, recently tentatively identified with Cyg X-3 (Hartman et al., 1976), which should be considered in this context. If the identification of this source is correct and if the ratio of its X-ray intensity to its  $\gamma$ -ray intensity is used to model the X-ray flux expected from  $\gamma$ 195+5, then  $\gamma$ 195+5 should be approximately as bright in X-rays as Cyg X-3. An upper limit on the X-ray flux from this location (Julien, 1976) is more than two orders of magnitude lower, ruling out this possibility. It should be noted that there are no established X-ray sources within  $\sim 6^\circ$  of  $\gamma$ 195+5 with the exception of a source recently reported by Forman, Jones, Tananbaum (1976). The longitude of this source is  $195.7^\circ$ ; a recent communication from the UHURU group (Forman, 1976) indicates a probable latitude of 1 to  $2^\circ$ , making the identification unlikely.

The region of the sky containing  $\gamma 195+5$  is shown in Fig. 6. Also shown are other features which are relevant to this discussion. The radio source, 4C+19.22, is located at the position labeled 1; positions 2, 3, and 4 are the next strongest non-thermal radio sources, 4C+19.21, 4C+19.23, and 4C+16.17, ordered according to intensity. Two supernova remnants known to be in this region are shown. The position of IC443, approximately  $6^\circ$  from the source, effectively rules out this identification. The X-ray source, 3U 0620+23, (Giacconi et al., 1974), conventionally associated with this remnant, is located about  $\frac{1}{2}^\circ$  off the upper edge of the figure. The other neighboring SNR, the so-called "Origem loop" (Berkuijsen, 1974) is probably unrelated to the source because of its location, more than  $4.5^\circ$  away, and its large,  $5^\circ$ , diameter.

The possibility that the source is due to cosmic ray interactions in a relatively nearby dense cloud has been examined. Lynds' catalogue of dark clouds (1962) shows no cloud at the position of the source and only relatively transparent (opacity class 1) clouds within  $3^\circ$  of the source. The 21 cm neutral hydrogen survey of Weaver and Williams (1973, 1974) shows a feature located near  $195^\circ$ ,  $+5^\circ$  at a relative velocity of  $-7$  km/s, which accounts for about  $1/3$  of the line profile in this region. The hydrogen column density of this feature is estimated to be  $\sim 10^{21}$   $\text{cm}^{-2}$ . If one uses the source function of Stecker (1973) the cosmic ray intensity in this cloud must be about 400 times greater than the local value in order to produce the observed  $\gamma$ -ray flux.



The recent announcement of a satellite galaxy (Simonson, 1975) located nearby has raised the possibility of an association (Cesarsky, Cassé, and Paul, 1976; and Bignami, Maccacaro, and Paizis, 1976). This association is improbable principally because of the mismatch in location and the fact that the  $\gamma$ -ray intensity is approximately two orders of magnitude greater than one expects from such a galaxy. The location of the core of the satellite galaxy is shown in Fig. 6, about  $3.7^\circ$  from the source or  $2.7\sigma$  using the combined uncertainty of both objects.

Simonson (1975) has estimated the mass of hydrogen in the core of this satellite galaxy to be in the range of  $(0.4 \text{ to } 1.6) \times 10^7 M_\odot$  and the distance from the Sun to be  $17 \pm 4$  kpc. Assuming the cosmic ray density to be as great as it is locally, a  $\gamma$ -ray flux of about  $5_{-3}^{+6} \times 10^{-8}$  (photons  $> 100 \text{ MeV}$ )/ $\text{cm}^2 \text{ s}$  would be expected from the interaction of cosmic rays with matter. This calculated flux is about 1/80 of the flux actually observed. Further, it is more reasonable to assume the cosmic ray density is lower than it is locally. Unless the cosmic ray flux is universal, which currently seems to be the less likely possibility, the cosmic ray density would be expected to be less in this smaller, less dense galaxy than in the local spiral arm of our galaxy because, as explained by Parker (1966, 1969) and discussed further by Bignami et al. (1975), the cosmic rays are held by the matter to which they are tied by the magnetic fields. The volume of the new galaxy is estimated to be in the range  $(0.5 \text{ to } 1) \times 10^{65} \text{ cm}^3$ , and therefore the average hydrogen gas density would be (1/4) to (1/8) that locally. Hence, the cosmic ray density would be expected to be lower. The best estimate of

the  $\gamma$ -ray flux may, therefore, very well be on the order of  $10^{-8}$  (photons  $> 100$  MeV)/(cm<sup>2</sup>sec) rather than  $5 \times 10^{-8}$  (photons  $> 100$  MeV/cm<sup>2</sup>sec), or, approximately 1/400 that which is observed.

The possibility that the source is associated with any external galaxy seems remote for the following reasons: If the emission is from a galaxy such as our own with a measured  $\gamma$ -ray luminosity to total mass ratio of  $\sim 5 \times 10^{-3}$  (photons  $> 100$  MeV)/g then the mass of the emitting galaxy would be given by  $M$  (in  $M_{\odot}$ ) =  $5 \times 10^{13} R^2$  where  $R$  is in Mpc. Under this hypothesis if the emission is from a twin of the Milky Way it must be located at a distance of 47 kpc, less than the distance to the Magellanic clouds. There is no evidence from optical, radio, or X-ray observations for such a massive nearby galaxy. If on the other hand, the  $\gamma$ -ray emission is enhanced relative to the mass of the external galaxy by some means, e.g. an unusual concentration of cosmic rays, then one would expect an accompanying enhancement of electron synchrotron emission in the radio region. Cen-A (NGC 5128) has been taken as an example of this latter possibility. The ratio of its total radio emission to the 100 MeV  $\gamma$ -ray emission as calculated by Grindlay (1975) on the basis of a Compton-Synchrotron model has been used to scale the observed  $\gamma$ -ray intensity of  $\gamma$ 195+5 to the radio region. On this basis, the total radio emission from  $\gamma$ 195+5 should exceed  $10^{-13}$  watts/m<sup>2</sup> or  $10^4$  Jy for an assumed band width of  $10^9$  Hz. All radio sources in this region have intensities which are smaller by more than a factor of  $10^3$ , effectively eliminating this possibility.



In summary, we regard it highly probable that  $\gamma$ 195+5 is galactic. A promising possibility is that it is an undiscovered pulsar. If so then a radio flux (at  $\sim 300 \text{ MHz}$ ) of greater than  $0.2 \text{ Jy}$  is predicted. Another possibility, which may be related to the pulsar possibility, is that the source is a site of an unusual concentration of cosmic rays,  $10^2$  to  $10^3$  times the local value, and these cosmic rays are interacting with a relatively local cloud of hydrogen with a column density  $\leq 10^{21} \text{ atoms/cm}^2$ . The positive correlation of this source with emission seen at other wavelengths remains an unattained goal. It is hoped that the discussion presented here will stimulate further efforts in this direction.

### C. Gould's Belt

The local system of stars, gas, and dust, known as Gould's Belt, is thought to be a thin disk of radius between 200 and 300 pc, tilted at about  $15^\circ$  to the galactic plane (Davies, 1960; Lynds, 1962; Goldstein and MacDonald, 1969). This system shows its greatest deviation from the plane of the galaxy in the direction of the galactic center (toward positive latitudes) and anticenter (towards negative latitudes). The fact that the observed  $\gamma$ -ray emission shows an asymmetry toward positive latitudes in the galactic center and toward negative latitudes in the anticenter has been noted as an indication of  $\gamma$ -ray production in the local system (Fichtel et al., 1975; Kniffen et al., 1975; Puget et al., 1976).

In Fig. 1, the extension of the  $\gamma$ -ray intensity contours toward negative latitudes is clear. With the exception of small, isolated

regions, the contours are restricted to latitudes below  $+10^\circ$ , while on the opposite side of the plane the contours reach  $-15^\circ$  over most of the longitude range. A similar pattern is seen in the 21 cm measurements of neutral hydrogen column densities (Davies, 1960; Fejes and Wesselius, 1973), the distribution of dark nebulae (Lynds, 1962), the line-of-sight dust concentration estimated from galaxy counts (Kiang, 1969), and the non-thermal continuum radio emission (Landecker and Wielebinski, 1970).

For  $\gamma$ -rays produced by cosmic ray--matter interactions in a region near the solar system, the cosmic ray density has been assumed to be the same as that observed locally. The expected  $\gamma$ -ray intensity can then be expressed as a function of the total gas column density  $N_H$  by

$$I_\gamma = 1.3 \times 10^{-25} N_H / 4\pi \text{ photons } (E > 100 \text{ MeV}) \text{ cm}^{-2} \text{ s}^{-1} \text{ sr}^{-1}$$

using the source function derived by Stecker (1973). The gas column density can be estimated either from reddening measurements using a dust-to-gas ratio determined independently (Puget, Ryter, and Serra, 1976) or from neutral hydrogen measurements with a correction for unseen gas such as molecular hydrogen. Since some evidence exists that the neutral hydrogen is correlated with the dust in the galaxy (Knapp and Kerr, 1974), these two approaches should be roughly compatible. Starting with the 21 cm data, the column density along  $b = -15^\circ$  is approximately  $2 \times 10^{21} \text{ atom cm}^{-2}$  (Davies, 1960; Fejes and Wesselius, 1973). Allowing a factor of two for unseen gas, the  $\gamma$ -ray intensity is calculated to be about  $4 \times 10^{-5} \text{ photons } (E > 100 \text{ MeV}) \text{ cm}^{-2} \text{ s}^{-1} \text{ sr}^{-1}$ . In figure 1, the lowest contour represents an intensity of approximately

$9 \times 10^{-5}$  photons ( $E > 35 \text{ MeV cm}^{-2}\text{s}^{-1}\text{sr}^{-1}$ , of which close to half is above 100 MeV. Since this contour also lies close to  $b = -15^\circ$ , the observed  $\gamma$ -ray intensity in the anticenter for this latitude is roughly  $4.5 \times 10^{-5}$  photons ( $E > 100 \text{ MeV cm}^{-2}\text{s}^{-1}\text{sr}^{-1}$ , consistent with the calculated value. At positive latitudes, both the  $2 \times 10^{21} \text{ atoms cm}^{-2}$  21 cm contour and the  $9 \times 10^{-5}$  photons ( $E > 35 \text{ MeV cm}^{-2}\text{s}^{-1}\text{sr}^{-1}$   $\gamma$ -ray contour are largely restricted to latitudes below  $+10^\circ$  in the anticenter. At these relatively high latitudes, these results support the concept that the dominant source of  $\gamma$ -rays is cosmic ray--matter interactions within the local system, Gould's Belt. The quantitative agreement of the calculation with the data also indicates that the local demodulated cosmic ray spectrum is representative of a region at least out to a distance of a few hundred parsecs.

Although correlations do appear on a broad scale between the  $\gamma$ -ray observations and other tracers of nearby matter, a comparison of details is not expected to reveal correlations on a small scale. As indicated by Fazio (1976), even the largest and densest gas clouds in the galaxy should not be detectable as localized sources with the sensitivity of the SAS-2 detector.

#### D. Other Possible Sources

In Fig. 1, the individual features which appear, except for the Crab and 195, +5 sources, are not statistically significant relative to the general background. Some mention should be made, however, of the feature near coordinates  $165^\circ, -39^\circ$ . This apparent high intensity

region lies near the limit of the SAS-2 exposure, so the number of  $\gamma$ -rays is small. 12  $\gamma$ -rays were detected in the region about these coordinates, where the expected contribution from diffuse radiation was about 3  $\gamma$ -rays. This improbable cluster of photons suggests that this region is a promising candidate for future study.

One other possible source in this region is the transient X-ray source, A0535 (Rosenberg et al., 1975) which had an X-ray intensity at maximum greater than the Crab with an extremely hard spectrum (Bradt et al., 1976). Although this source is only  $4\frac{1}{2}^\circ$  from the Crab the additional observation of a 104 second modulation of the X-ray intensity provides a potential means of source identification in the presence of background from the Crab and the galactic ridge. A search of the SAS-2 data for this source with trial periods in the range of 102.8 to 104.9 seconds was made. No statistically-significant evidence for a sharply peaked phase modulation was seen and a 95% confidence upper limit for the  $\gamma$ -ray intensity from this source during the time of the SAS-2 observations can be set at  $2.0 \times 10^{-6}$  (photons  $> 100$  MeV)  $\text{cm}^{-2}\text{s}^{-1}$ .

### III. SUMMARY

The overall view of the anticenter region presented here is one in which two strong localized sources, the Crab nebula and  $\gamma$ 195+5, are clearly evident above a diffuse emission. This diffuse emission is generally strongest on the plane and shows an asymmetry in latitude which correlates with Gould's Belt. Certain aspects of these features are worth particular emphasis.

1. The radiation from the Crab nebula is mostly pulsed with the pulsed fraction increasing with energy.

2. The intensity of the radiation in the main and interpulse peaks is approximately equal.

3. The total Crab  $\gamma$ -ray intensity above 100 MeV is  $(3.7 \pm 0.8) \times 10^{-6}$  photons  $\text{cm}^{-2} \text{s}^{-1}$  with a differential number index,  $\alpha$ , equal to  $2.25^{+0.40}_{-0.35}$ .

4. A source whose position is  $l = 194.9 \pm 1.5^\circ$ ,  $b = 4.9 \pm 2.2^\circ$  (95% confidence) has an intensity above 100 MeV of  $(4.3 \pm 0.9) \times 10^{-6}$  photons  $\text{cm}^{-2} \text{s}^{-1}$ , approximately the same as the Crab intensity. However, the spectrum appears harder, being consistent with a  $\pi^0$  plus bremsstrahlung origin or a power law with spectral index less than 1.9 (95% confidence).

5. Unlike the Crab there is no obvious radio counterpart to  $\gamma 195+5$ . If this source is due to a radio pulsar then a scale factor obtained from the known  $\gamma$ -ray emitting pulsars predicts a radio intensity of 0.2 to 1.4 Jy.

6. The emission of  $\gamma 195+5$  is probably not from an external galaxy. This conclusion was reached by considering the consequences of either emission from an ordinary galaxy such as our own or emission from an unusually active galaxy such as Cen A. Emission from the satellite galaxy of Simonson (1975) is also ruled out.

7. A 21 cm neutral hydrogen feature with an estimated column density of  $\sim 10^{21} \text{cm}^{-2}$  does correlate with the position of  $\gamma 195+5$ . However, the cosmic ray intensity in this cloud must be several hundred times the local value to produce the observed flux.

8. Although not statistically significant, an excess near coordinates  $165^\circ$ ,  $-39^\circ$  is a promising candidate for future  $\gamma$ -ray observations.

9. The diffuse radiation correlates rather well with the local matter distribution known as Gould's Belt in both position and expected  $\gamma$ -ray intensity. The correlation in intensity was established using the local demodulated cosmic ray spectrum, and therefore the  $\gamma$ -ray measurements serve in some sense to support the constancy of the cosmic ray intensity to distances of a few hundred parsecs from the earth.

#### IV. ACKNOWLEDGMENTS

We wish to express our thanks to the many people who made SAS-2 possible. In particular with regard to the experiment itself, we wish to acknowledge the dedication and expertise of Mr. R. Ross, the detector engineer, Mr. C. Ehrmann, the electronics engineer, Mr. W. Cruickshank, the spark chamber systems mechanical engineer, Mr. M. Calabrese, the structural engineer, Ms. A. Fitzkee, the thermal engineer, Mr. S. Derdeyn, the experiment manager, and the many others whose efforts are sincerely appreciated. We also wish to express our gratitude to Ms. M. Townsend, the SAS Project Manager, and [redacted] aff, and to Mr. H. Riblet and his entire team at the Johns Hopkins Applied Physics Laboratory who were responsible for the SAS-2 spacecraft control section. We congratulate the San Marco launch team of Centro Ricerche Aerospaziali for providing SAS-2 with a successful launch. For their efforts in the experimental calibration, we thank the Radiation Physics Branch of the National Bureau of Standards and the Hallendienst staff of the Deutsches Elektronen-Synchrotron. We also acknowledge the work

of Dr. Hakki Ogelman, Middle East Technical University, Ankara, during the preliminary phases of some of this work while he was at Goddard Space Flight Center.



## FIGURE CAPTIONS

- Fig. 1 - Contour map of  $\gamma$ -ray intensities observed by SAS-2 at energies above 35 MeV in the galactic anticenter region. The contour lines represent 75%, 66%, 57%, 48%, 39%, 30%, and 21% of the maximum intensity, which is  $4.25 \times 10^{-4}$  photons ( $E > 35$  MeV)  $\text{cm}^{-2}\text{s}^{-1}\text{sr}^{-1}$ . The 66% and 21% contour lines are slightly darker than the others. The apparent positions of the two maxima near  $185^\circ, -6^\circ$  and  $195^\circ, +5^\circ$  differ slightly from these coordinates principally due to the presence of the diffuse emission from the galactic plane, as discussed in the text. The dashed line is the limit of the SAS-2 exposure in this region.
- Fig. 2 - Distribution of  $\gamma$ -ray arrival times in fractions of a pulse period for  $\gamma$ -rays above 35 MeV from the direction of PSR 0531+21. M and I give the locations of the predicted main and interpulse times determined from radio observations (Rankin, private communication). The dashed line shows the estimated contributions from the celestial and galactic diffuse emission and the source near  $195^\circ, +5^\circ$ .
- Fig. 3 - Energy spectrum of the pulsed  $\gamma$ -ray emission from PSR 0531+21. The line  $1.0 E^{-1.1} \text{ keV cm}^{-2}\text{s}^{-1}\text{keV}^{-1}$  with  $E$  in keV connects the SAS-2 results near 200 MeV with the X-ray results near 10 keV.
- Fig. 4 - Intensity profiles in latitude and longitude near coordinates  $195^\circ, +5^\circ$ . The longitude bins are  $2\frac{1}{2}^\circ \times 10^\circ$ . The latitude bins are  $2^\circ \times 10^\circ$ . Each point represents the net intensity after an estimate of the diffuse galactic and celestial emission has been subtracted.



Fig. 5 - Distribution of  $\gamma$ -ray arrival times in fractions of a pulse period for  $\gamma$ -rays above 35 MeV from the region of 195+5, assuming the period and period derivative shown. Due to the number of trial periods and the use of a period derivative, the result must be considered tentative.

Fig. 6 - The region of the sky containing  $\gamma$ 195+5, shown in celestial coordinates. The points marked 1, 2, 3, and 4 are the four strongest radio sources within the  $\gamma$ 195+5 error box: 4C+19.22, 4C+19.21, 4C+19.23, and 4C+16.17. The position of the possible satellite galaxy is taken from Simonson (1975).

## REFERENCES

- Albats, P., Frye, G. M., Jr., Zych, A. D., Mace, O. B., Hopper, V. D.,  
and Thomas, J. A. 1972, *Nature* 240, 221.
- Bennett, A. S. 1962, *Mem. Roy. Astron. Soc.*, 68, 163.
- Bennett, K., Bignami, G. F., Boella, G., Buccheri, P., Burger, J. J.,  
Cuccia, A., Hermesen, W., Higdon, J., Kanbach, G., Koch, L.,  
Lichti, G. G., Masnou, J., Meyer-Hasselwander, H. A., Paul, J. A.,  
Scarsi, L., Shukla, P. G., Swanenburg, B. N., Taylor, B. G., and  
Wills, R. D. 1976, *Proc. 2nd Int. Gamma-Ray Symp.*, GSFC X-662-76-154.
- Berkuijsen, E. M. 1974, *Astron. & Astrophys.*, 35, 429.
- Bignami, G. F., Maccacaro, T., and Paizis, C. 1976, *Astron. & Astrophys.*  
in press.
- Bignami, G. F., Fichtel, C. E., Kniffen, D. A., and Thompson, D. J. 1975,  
*Ap. J.*, 199, 54.
- Bradt, H., Moyer, W., Buff, J., Clark, G. W., Duxsey, R., Hearn, D.,  
Jerrigan, G., Joss, P. C., Laufer, B., Lewin, W., Li, F., Matilsky, T.,  
McClintock, J., Primini, F., Rappaport, S., and Schnopper, H. 1976  
*Ap. J. (Letters)*, 204, 167.
- Corning, R., Ramsden, D., and Wright, P. J. 1971, *Nature*, 232, 99.
- Cesarsky, C. J., Cassé, M., and Paul, J. 1976, *Astron. & Astrophys.* 48, 481.
- Davies, R. D. 1960, *Ap. J.*, 120, 35.
- Davies, J. G., Lyne, A. G., and Seiradakis, J. H. 1973, *Nature Phys.*  
*Sci.*, 244, 84.
- Derdeyn, S. M., Ehrmann, C. H., Fichtel, C. E., Kniffen, D. A., and  
Ross, R. W. 1972, *Nucl. Instr. and Methods*, 98, 557.
- Dixon, R. S. 1970, *Ap. J. Suppl.*, 20, 1.
- Fazio, G. 1976, *Proc. 2nd Int. Gamma-Ray Symposium*, NASA-GSFC,  
X-662-76-154.

- Fejes, I., and Wesselius, P. R. 1973, *Astron. & Astrophys.*, 24, 1.
- Fichtel, C. E., Hartman, R. C., Kniffen, D. A., Thompson, D. J.,  
Bignami, G. F., Ögelman, H., Özel, M. E., and Tümer, T. 1975,  
*Ap. J.*, 198, 163.
- Fishman, G. J., Harnden, F. R., Jr., Johnson, W. N. III, and Haymes,  
R. C. 1969, *Ap. J. (Letters)*, 158, L61.
- Forman, W., Jones, C., and Tananbaum, H. 1976, *Ap. J. (Letters)*,  
206, L29.
- Forman, W. 1976, private communication.
- Giacconi, R., Murray, S., Gursky, H., Kellogg, E., Schreier, E.,  
Matilsky, T., Koch, D., and Tananbaum, H. 1974, *Ap. J. Suppl.*,  
27, 37.
- Goldstein, S. J., Jr., and MacDonald, D. D. 1969, *Ap. J.*, 157, 1101.
- Greisen, K., Ball, S. E., Jr., Campbell, M., Gilman, D., and Strickman,  
M. 1975, *Ap. J.*, 197, 471.
- Grindlay, J. E. 1975, *Ap. J.*, 199, 49.
- Hartman, R. C., Fichtel, C. E., Kniffen, D. A., Lamb, R. C., Thompson,  
D. J., Bignami, G. F., Ögelman, H., Özel, M., and Tümer, T. 1976,  
*Proc. 2nd Int. Gamma-Ray Symposium, NASA-GSFC, X-662-76-154*.
- Helmken, H., 1975, *Proc. 14th International Cosmic Ray Conf.* 1, 128.
- Helmken, H. and Hoffman, J. 1973, *Proc. 13th International Cosmic Ray  
Conf.*, 1, 31.
- Julien, P., 1976, private communication.
- Kettenring, G., Mayer-Hasselwander, H. A., Pfefferman, E., Pinkau, K.,  
Rothermel, H., and Sommer, M. 1971, *Proc. 12th International Conf.  
on Cosmic Rays*, 1, 57.

- Kiang, T. 1969, Dunsink Observatory Publications, 1, #5.
- Kinzer, R. L., Share, G. H., and Seeman, N. 1973, Ap. J., 180, 54.
- Knapp, G. R., and Kerr, F. J. 1974, Astron. & Astrophys., 35, 361.
- Kniffen, D. A., Hartman, R. C., Thompson, D. J., Bignami, G. F.,  
Fichtel, C. E., Ügelman, H., and Tümer, T. 1974, Nature, 251,  
397.
- Kniffen, D. A., Bignami, G. F., Fichtel, C. E., Hartman, R. C.,  
Ügelman, H., Thompson, D. J., Üzel, M. E., and Tümer, T., 1975,  
Proc. 14th Int. Cosmic Ray Conf., Munich, 1, 100.
- Kurfess, J. D. 1971, Ap. J. (Letters), 168, L39.
- Landecker, T. L., and Wielebinski, R. 1970, Austral. J. Phys  
Astrophys. Suppl. 16.
- Laros, J. G., Matteson, J. L., and Pelling, R. R., 1973, Nature  
Phys. Sci., 246, 109.
- Lynds, B. T. 1962, AP. J. Suppl., 1, 1.
- McBreen, B., Ball, S. E., Jr., Campbell, M., Greisen, K., and Koch, D.  
1972, Ap. J., 184, 571.
- Mills, B. Y., Slee, O. B., and Hill, E. R. 1960, Austral. J. Phys.,  
13, 676.
- Ügelman, H. B., Fichtel, C. E., Kniffen, D. A., and Thompson, D. J.  
1976, Ap. J., 209 (in press).
- Orwig, L. E., Chupp, E. L., and Forrest, D. J. 1971, Nature Phys.  
Sci. 231, 171.
- Parker, E. N. 1966, Ap. J., 145, 811.
- Parker, E. N. 1969, Space Science Rev., 9, 654.

- Parlier, B., Agrinier, B., Forichon, M., Leray, J. P., Boella, G.,  
Maraschi, L., Buccheri, R., Robba, N.R. and Scarsi, L. 1973,  
Nature Phys. Sci., 242, 117.
- Puget, J. L., Ryter, C., and Serra, G. 1976, 2nd Int. Gamma-Ray  
Symposium, NASA-GSFC, X-662-76-154.
- Puget, J. L., Ryter, C., Serra, G., and Bignami, G. 1976, Astron.  
& Astrophys. (to be published).
- Seiradakis, J. H. 1976, Proc. 2nd Int. Gamma-Ray Symposium, NASA-GSFC,  
X-662-76-154.
- Simonson, S. C. III 1975, Ap. J. (Letters), 201, L103.
- Stecker, F. W. 1970, Ap. and Space Sci., 6, 377.
- Stecker, F. W. 1973, Ap. J., 185, 499.
- Taylor, J. H. and Manchester, R. N. 1975, Astron. J., 80, 794.
- Thomas, R. M., and Fenton, K. B. 1975, Proc. 14th International  
Cosmic Ray Conference, Munich, 1, 188.
- Thompson, D. J., Fichtel, C. E., Kniffen, D. A., and Ügelman, H. B.  
1975, Ap. J. (Letters), 200, L79.
- Thompson, D. J., Fichtel, C. E., Kniffen, D. A., Lamb, R. C., and  
Ügelman, H. B. 1976, Ap. Letters (in press).
- Weaver, H., and Williams, D.R.W. 1973, Astron. & Astrophys. Suppl.,  
8, 1.
- Weaver, H., and Williams, D.R.W. 1974, Astron. & Astrophys. Suppl.,  
17, 1.
- Weisskopf, M. C., Cogen, G. G., Kestenbaum, H. L., Long, K. S., Novick,  
R., Wolff, R. W. 1976, Columbia Astrophysics Lab. Contribution  
No. 125 (preprint).

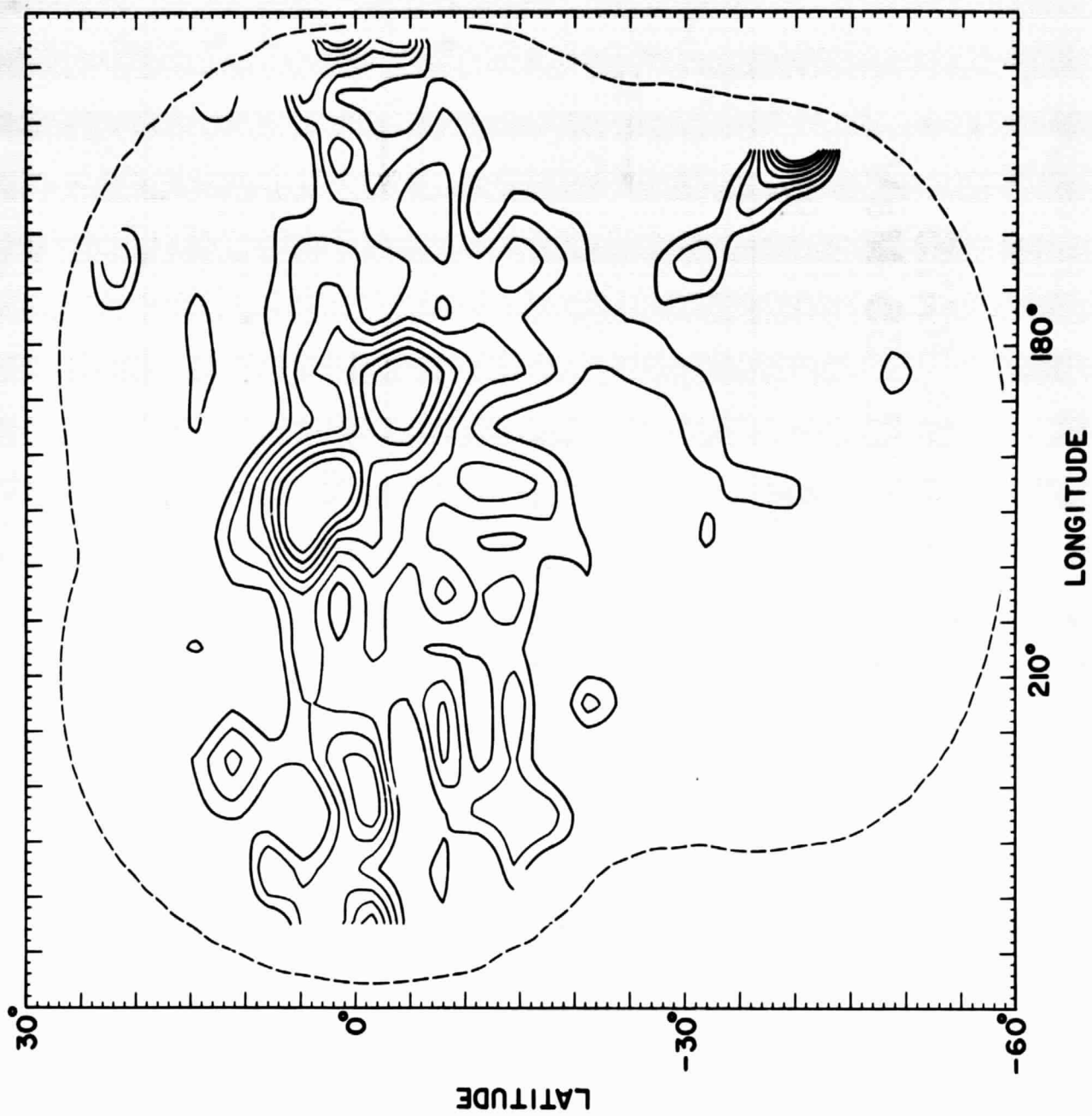


Fig.1

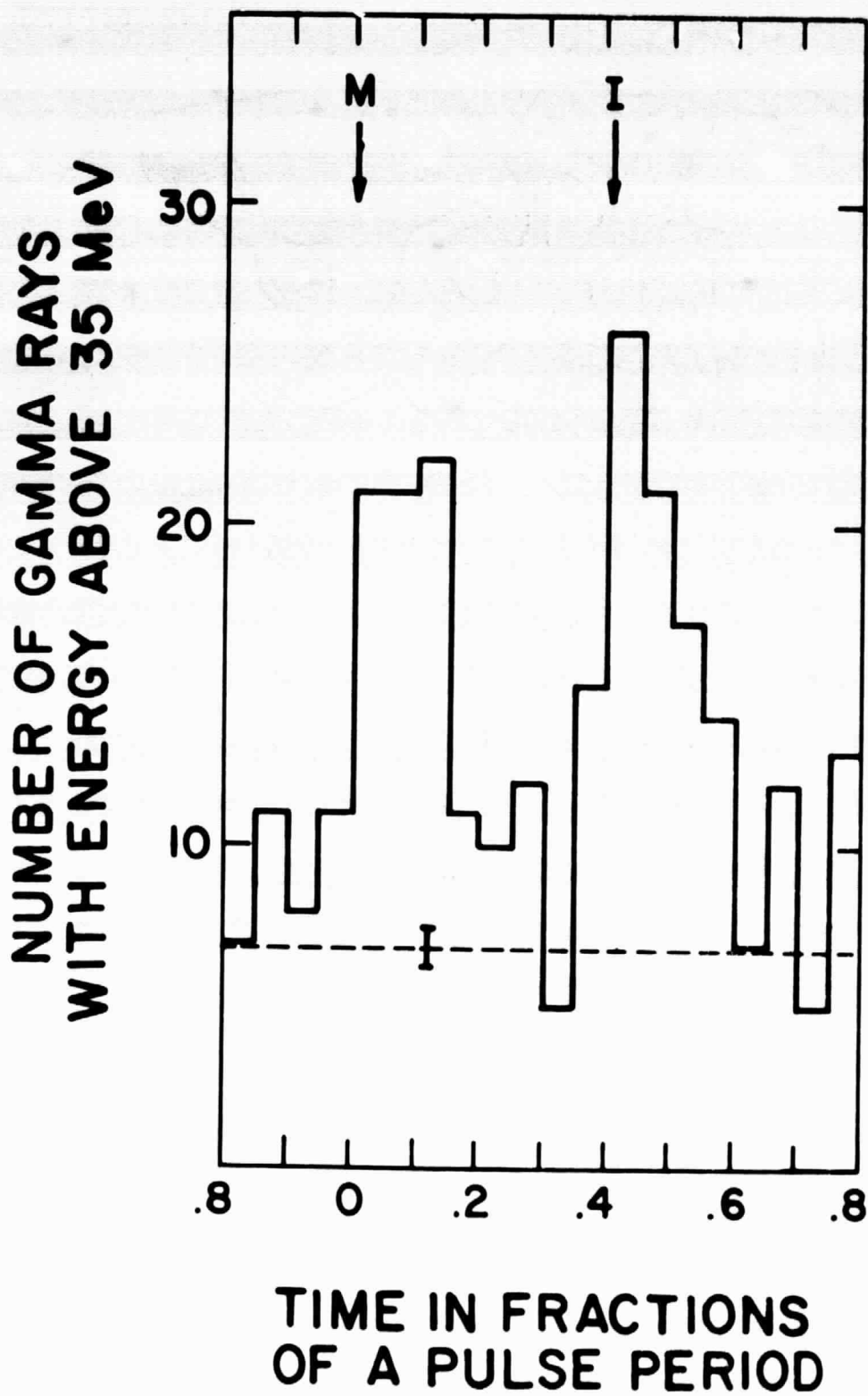


Fig.2

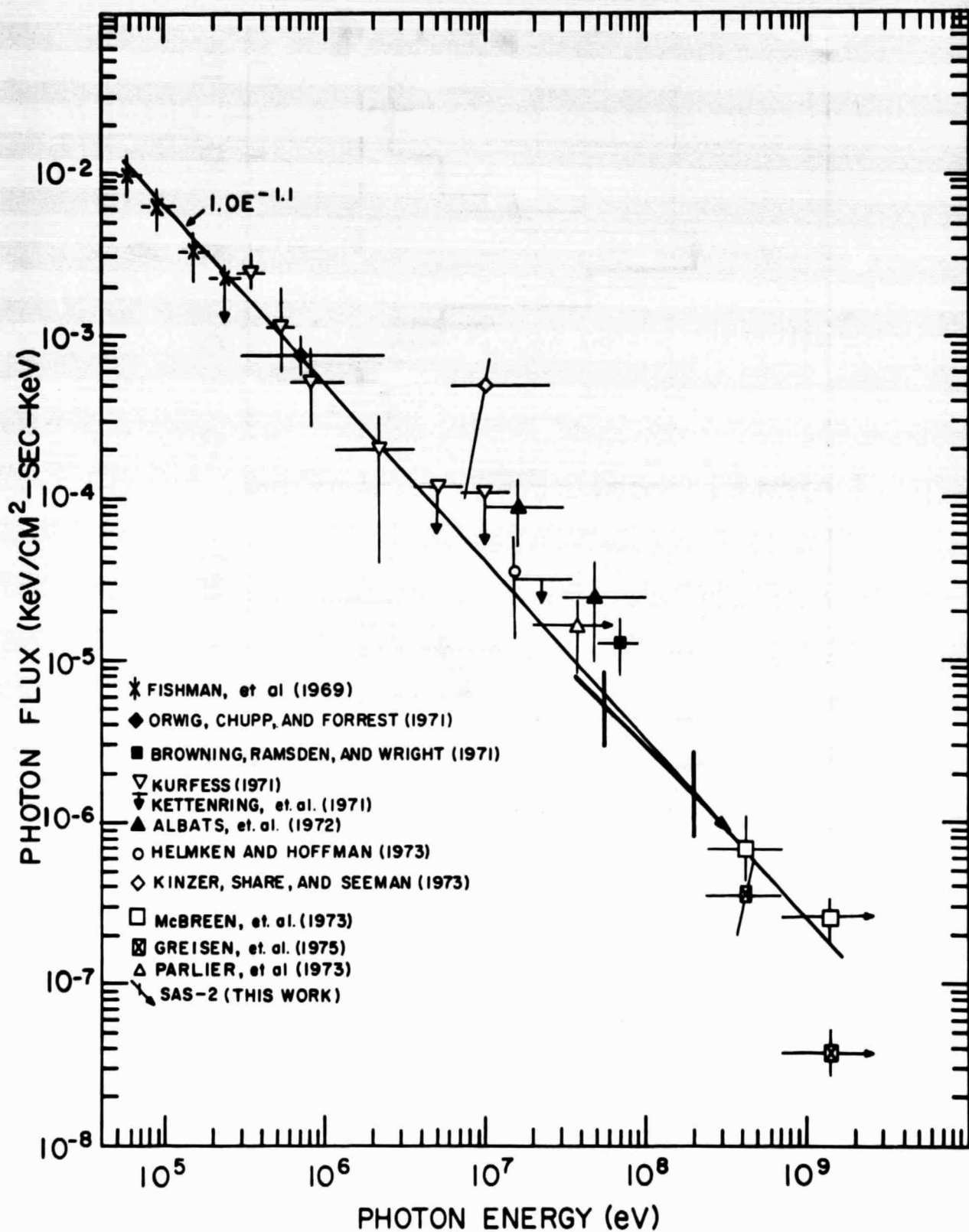


Fig.3



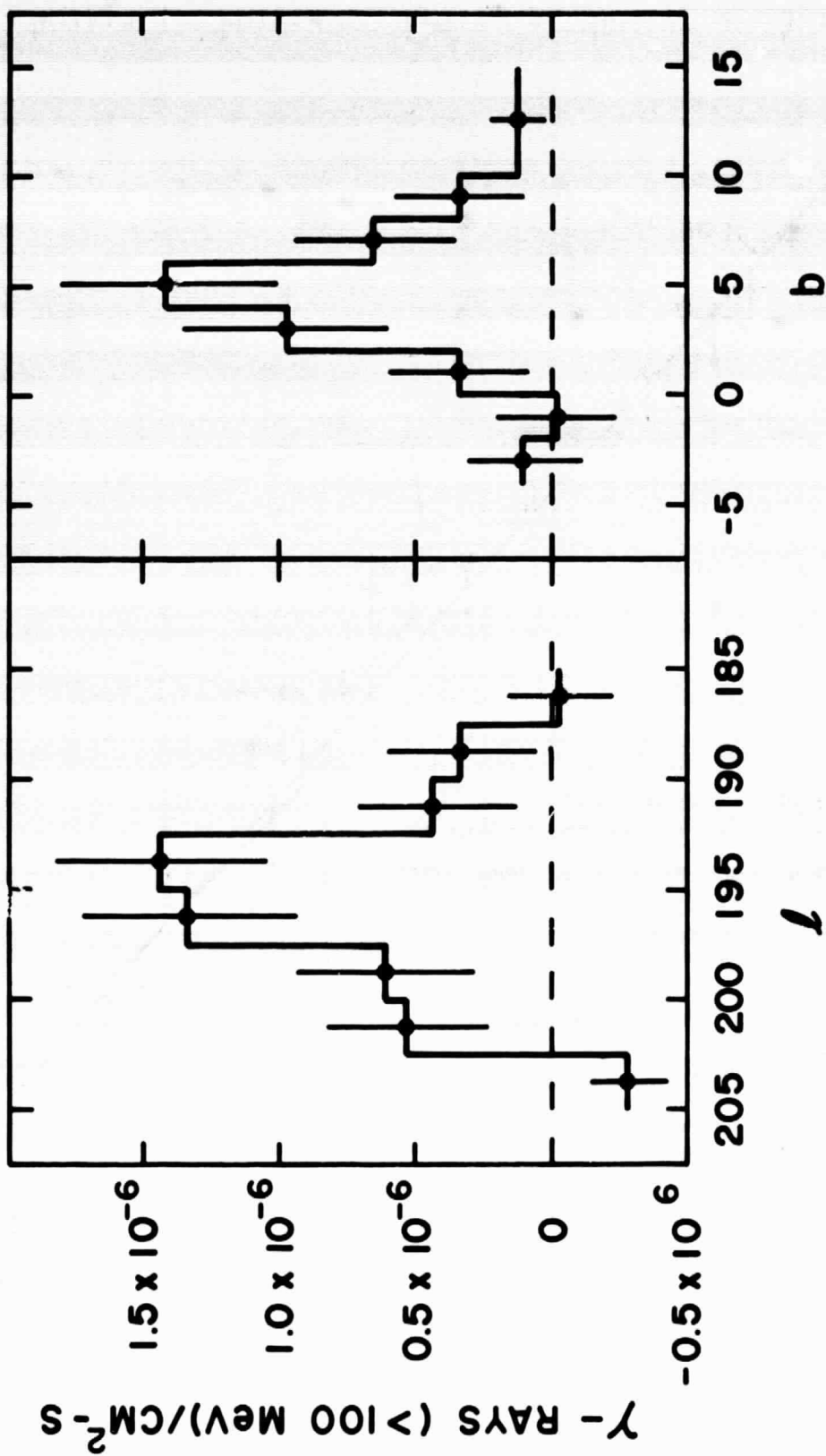


Fig.4

$P_0 = 59.0074 \text{ SEC}$

$\dot{P} = 2.23 \times 10^{-9}$

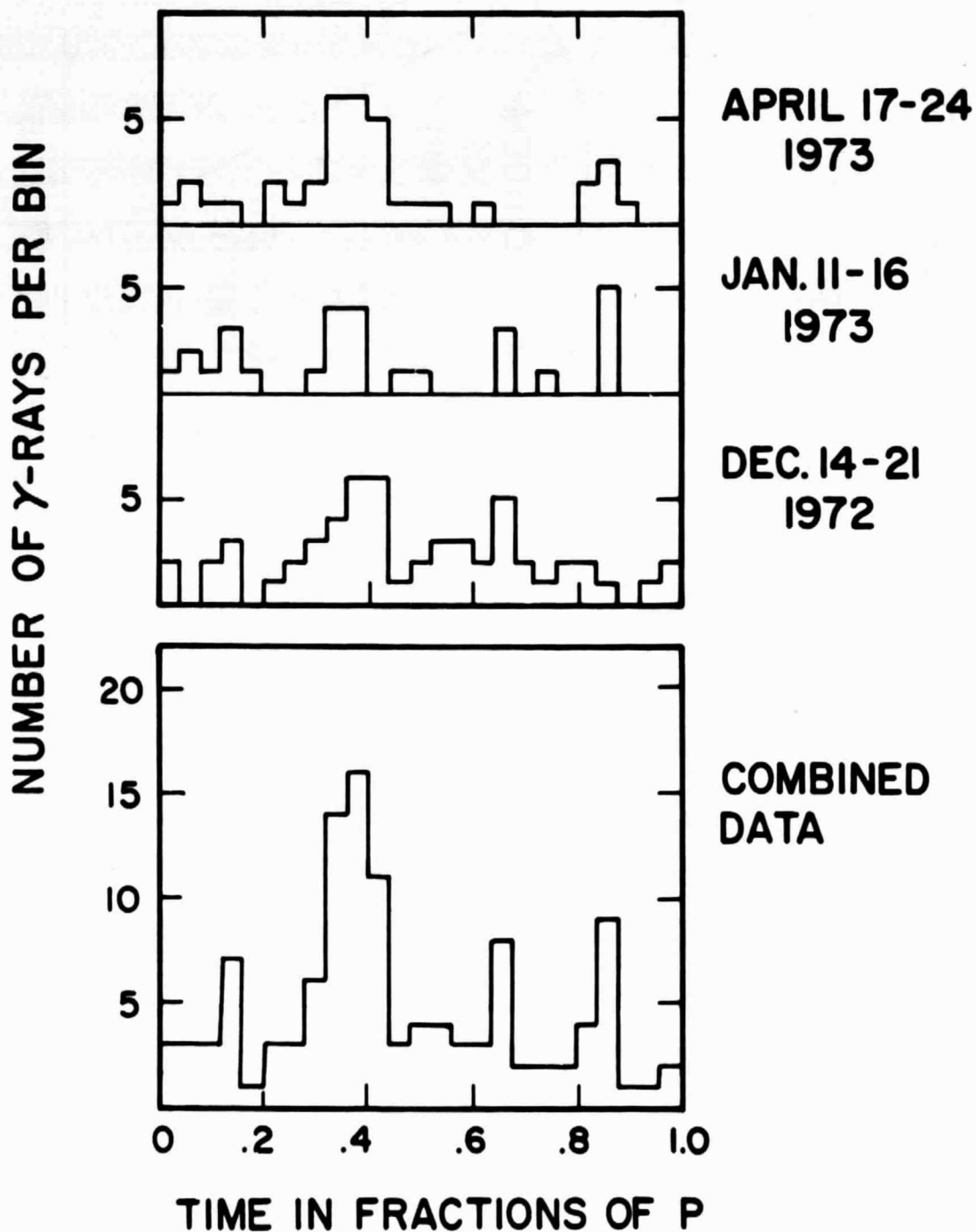


Fig.5

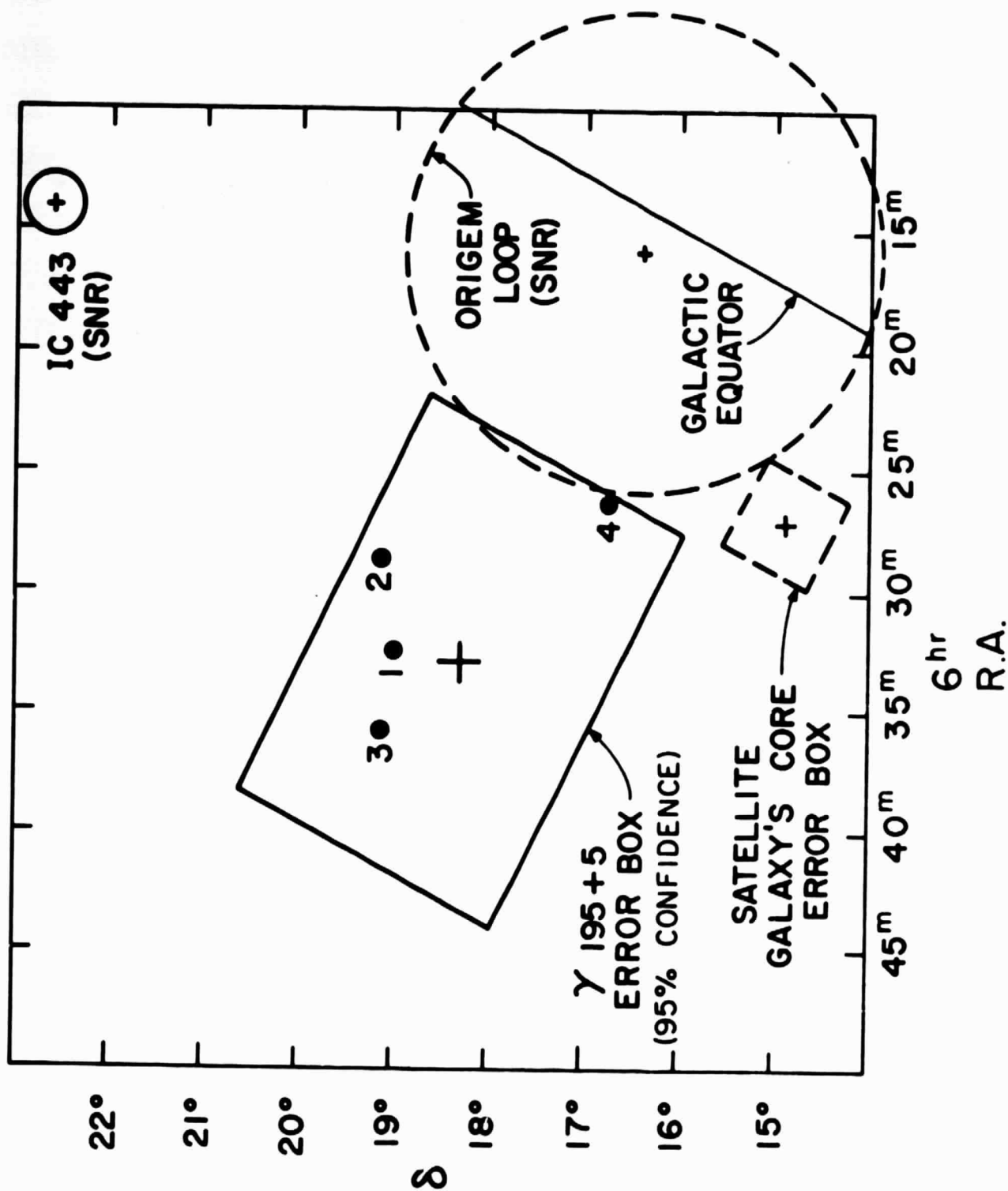


Fig. 6